ISSN: 2182-2069 / E-ISSN: 2182-2077

Designing Wireless Sensor Network Data Based Machine Learning Approach for Accurate Human Activity Recognition

Haydar Abdulameer Marhoon[1*], Atheer Y. Oudah[2], Naseer Ali Hussien[3], and Alubady Raaid[4]

[1*]Information and Communication Technology Research Group, Scientific Research Center, Al-Ayen University, Thi-Qar, Iraq; College of Computer Sciences and Information Technology, University of Kerbala, Karbala, Iraq. haydar@alayen.edu.iq, https://orcid.org/0000-0002-2711-1857

[2]Information and Communication Technology Research Group, Scientific Research Center, Al-Ayen University, Thi-Qar, Iraq; Department of Computer Sciences, College of Education for Pure Science, University of Thi-Qar, Iraq. atheer@alayen.edu.iq, https://orcid.org/0000-0003-0867-7203

[3]Information and Communication Technology Research Group, Scientific Research Center, Al-Ayen University, Thi-Qar, Iraq. naseerali@alayen.edu.iq, https://orcid.org/0000-0002-5792-6141

[4]Information and Communication Technology Research Group, Scientific Research Center, Al-Ayen University, Thi-Qar, Iraq; College of Information Technology, University of Babylon, Babil, Iraq. alubadyraaid@alayen.edu.iq, https://orcid.org/0000-0001-9748-2541

Received: December 14, 2024; Revised: January 20, 2025; Accepted: January 30, 2025; Published: February 28, 2025

Abstract

Human activity recognition (HAR) using a Wireless Sensor Network (WSN) is essential for understanding human behavior and predicting future actions. With HAR, smartphones, and classification models are important aspects. This study explores the use of WSNs for classifying human activities by analyzing time series data captured using wireless devices. This paper aims to design an intelligent model for classifying human activity from WSN data. This paper combines multivariate dynamic mode decomposition (MDMD), Hankel Block (HB), and an ensemble classifier for classifying physical human activity. The MDMD decomposes time series data into principal modes, from which features are extracted for analysis and classification. The Hankel matrix enhances the estimation of hidden oscillatory modes when integrated with MDMD. Ensemble classifiers are employed to classify the extracted feature. The proposed model's performance is evaluated on three datasets, UCI-HAR, Opportunity, and WISDM. The obtained results proved that the proposed model is superior to competing models, and it can be deployed in WSN to support different real-time applications.

Keywords: Human Activity Recognition, MDMD, WSN.

Journal of Internet Services and Information Security (JISIS), volume: 15, number: 1 (February), pp. 385-400.
DOI: *10.58346/JISIS.2025.I1.025*

*Corresponding author: Information and Communication Technology Research Group, Scientific Research Center, Al-Ayen University, Thi-Qar, Iraq; College of Computer Sciences and Information Technology, University of Kerbala, Karbala, Iraq.

1 Introduction

Wireless Sensor Networks (WSNs) based on human Activity Recognition have been used in different applications including smart homes, security, healthcare, and industrial automation (Faye et al., 2016). Traditional HAR methods depend on vision-based systems, which often face limitations such as accuracy, occlusions, and environmental limitations. In contrast, WSN-based HAR systems offer advanced data processing and classification techniques.

The demand for more advanced IoT applications has been raised to enhance people's daily lives (Raj et al., 2024; Rahdar et al., 2024). Recently, IoT applications have opened new advanced avenues of research in the field of human activity analysis and recognition from sensor data (Menaka et al., 2022; Abuhoureyah et al., 2024; Wang et al., 2024). In recent years, smart devices like phones and smartwatches have attracted great popularity (Hussain et al., 2024; Saw & Wong, 2023; Bursa et al., 2023). Those smart devices are combined with advanced motion sensors such as accelerometers, gyroscopes, magnetometers, and GPS which are utilized in various applications, including Human Activity Recognition (HAR) models (Ding et al., 2023; Duan et al., 2024; Gao et al., 2021).

Human activity recognition (HAR) via WSN is rapidly advancing by applying more accurate machine learning models (Moya Rueda et al., 2018). Human activity from smartphones based on machine learning has been used in various applications including rehabilitation, healthcare (Armstrong & Tanaka, 2025), and sports as well as automated observation to forecast fall detection of elderly people (Ahmed & Pandey, 2024; Singh et al., 2020; Zhao et al., 2018; Ordóñez & Roggen, 2016; Xu et al., 2019). Mainly, physical human activity recognition is carried out using images, videos, and time series, however, the time series-based approach is the most common procedure to identify physical human activity (Ahmadian et al., 2024; Patricia et al., 2024; Jethanandani et al., 2020).

Unsupervised learning-based approaches have been employed in which only unlabelled data was used to train the model. Lu et al., (2017) used a density for clustering to classify human activity (Zahin et al., 2019). Bai et al., (2019) suggested a deep learning model-based variational autoencoder named Motion2Vector. In that study, the model learned the features of activities with unlabelled samples and then clustered the activities using the Euclidean distance metric. Ma et al., (2021) combined a CNN-BiLSTM autoencoder with K-means. Where CNN-BiLSTM autoencoder was used to form feature representation, then the K-means was applied to allocate labels for samples and train the deep learning model. Xia et al., (2020) proposed an unsupervised human activity recognition method (Kumar et al., 2023). Moya Rueda et al., (2018) proposed a semi-supervised learning model for HAR. In that study, an adversarial autoencoder employing convolutional networks was adopted for feature extraction. The authors combined unlabelled samples and a small amount of labeled samples to train a model to recognize human activities. Study in (Ordóñez & Roggen, 2016) a domain adaptation (UDA) model based on features was designed to identify human activities from sensory data that were collected using smartphones (Hur et al., 2018). In another study, an unsupervised online domain adaptation model was suggested in (Patricia et al., 2024).

Several multivariate decomposition techniques have been developed to analyze time series data such as Multivariate empirical mode decomposition (MEMD), empirical mode decomposition, and Dynamic mode decomposition (DMD) (Vasconcelos Filho & dos Santos, 2019; Zhang et al., 2023). DMD has been widely employed in several fields due to its dynamic ability to extract important features from signals. The DMD classifies the dynamics of input signals by generating a proxy dynamical matrix (PDM). Then, it decomposed the PDM into modes to pull out the dynamical features hidden in the signal. However, the DMD has some limitations for example, If the time series is too noisy as sensor data, the eigenvalues generated by DMD are influenced by the noise of signal (Reddy & Pachori, 2024; Schmid, 2010). To solve the above problems, a novel multivariate DMD (MDMD) model has been proposed to analyze sensor data (Kang et al., 2019).

We summarised the significant contributions of the study as follows:

- We developed an effective feature extraction model that integrates MDMD with the Hankel matrix. The advantage of integrating the DMDM with the Hankel matrix is to improve the recognition capability of the model as the Hankel matrix expands the number of estimated modes.
- We employed several statistical metrics including Shap to study the behavior of the model based on different types of features.
- Three real-world datasets are employed for performance evaluation, and the results are compared with the state-of-the-art human recognition models. Moreover, the proposed model is compared with other ensemble classifiers to validate its advantages.

The rest of the paper is organized as follows: Section 2 reviews the previous studies, Section 3 describes the methodology, and Section 4 describes the experimental results. Section 5 discusses the main findings. Section 6 summarizes the conclusion and the future scope.

2 The Proposed Methodology and Material

In this section, we explained the proposed approach for HAR. Three main phases are considered in this paper: In the first phase, the MDMD is employed to analyze and decompose the input time-series data. This approach helps to analyze the input data and to reveal linear and nonlinear dynamic characteristics of the input data. The MDMD is combined with the Hankel algorithm to expand the number of estimated modes. In the second phase, a set of features is extracted from each MDMD mode. This step aims to extract and find highly recognized characteristics to identify human activities. In the third phase, a dynamic ensemble model is designed to classify the extracted features into different classes. The proposed ensemble model combines the outputs of multi-base classification models using a novel strategy. Finally, the proposed model is evaluated on three real public datasets. The overall schema of the proposed method is presented in Figure 1.

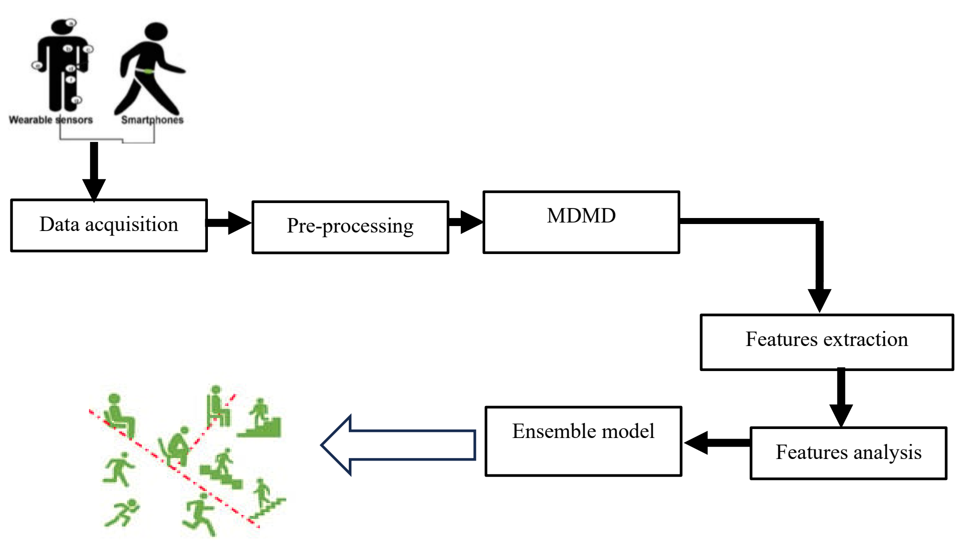

Figure 1: The Details of the Proposed Model for Human Activity Recognition

Data Segmentation

In this paper, the sensory data collected from three datasets is segmented, and each segment is passed through MDMD. We adopted our previous study (Diykh et al., 2023) to segment the data in this paper. We selected different window sizes for each dataset. As a result, the window sizes were set as 10s, 5.21s, and 3s for the WISDM, and UCI-HAR Opportunity datasets respectively.

Multivariate Dynamic Mode Decomposition

The dynamic mode decomposition (DMD) was improved and extended by (Reddy & Pachori, 2024). In that study, they suggested MDMD to resolve the limitations included in DMD. In this paper, each data sample is passed through MDMD to decompose it into modes to extract extracting both linear and nonlinear dynamic characteristics from each segment. Suppose a human activity data signal $S = \{s^i(n): i = 1, \ . \ . \ . \ , l; \quad n = 1, \ . \ . \ . \ , m\}$ where l refers to multivariable and m denotes the samples. Figure 2 shows different activity plots. The sensory data was used as an input into the MDMD. The main steps of MDMD are described as follows:

1. Step 1: we calculated the trajectory matrix M^i independently for each variable l in the time series S and it is given as follows (Eq. 1):

$$M^i = \begin{bmatrix} S^i(1) & S^i(2) & .. \ .. & S^i(j) \\ S^i(2) & S^i(3) & .. \ .. & S^i(h+1) \\ :: & :: & :: \ :: & :: \\ S^i(h) & S^i(h+1) & .. \ .. & S^i(m) \end{bmatrix} \qquad (1)$$

Where i is the variable number, h is an embedding dimension, $j = m - h + 1$. The trajectory matrix of each variable is stacked and concatenated in $M = [M^1, M^2, \ldots \ldots, M^l]$. The dimension of M is $hXjl$. In addition, each column represents a segment. We suppose the total number of segments in the trajectory matrix M is k. As a result, it can be represented as $M^m = [S_1, S_2, \ldots \ldots, S_k]$, where k is equal to jl.

2. The error across all segments of M^m is minimized. The matrix $M^m = [S_1, S_2, \ldots \ldots, S_k]$ is shifted by one segment to separate it into two matrixes which are defined as $R = [S_1, S_2, \ldots \ldots, S_{k-1}], Y = [S_2, S_3, \ldots \ldots, S_k]$.
3. We calculated the high-dimensioned matrix A. The matrix A is computed as (Eq. 2 & 3).

$$A = YR^{-1} \qquad (2)$$

$$R = U \sum V * \qquad (3)$$

Where R is computed using singular mode decomposition, $\sum$ is the diagonal matrix of eigenvalues. The U, V are the eigenvectors. The eigenvalues and eigenvectors of corresponding modes.

4. We projected the matrix A onto U to find a low-rank matrix. It is given as follows (Eq. 4):

$$A_I = U^T A U = U^T Y V \sum^{-1} \qquad (4)$$

5. The computation of the eigenvalue of the matrix A is obtained as (Eq. 5)

$$A_I W = W \wedge \qquad (5)$$

Each column in W represents an eigenvector of A_I and $\wedge$ is a diagonal matrix that contains the eigenvalues of the matrix A_I.

6. We calculated the dynamic modes $\pitchfork$ from each column of the eigenvectors W. Figure 3 shows the corresponding mode for each activity (Eq. 6).

$$\pitchfork = YV\sum W \tag{6}$$

7. We computed the normalized embedded matrix C using $\pitchfork$ (Eq. 7).

$$C = \frac{(\pitchfork^T \pitchfork}{j} \tag{7}$$

8. The resulting matrix C in Step 7 contains redundant information. To extract the significant components, we applied eigenvalue decomposition on the matrix C. As a result, we obtained eigenvalues γ, and eigenvectors μ as follows (Eq. 8):

$$[\mu, \gamma] = eig(C) \tag{8}$$

9. The eigenvectors are associated with huge eigenvalues corresponding to the time series data, so we reduce the dimensionality using the principal component (PC) while maintaining the relevant information as (Eq. 9).

$$PC = \pitchfork\ (\mu) \tag{9}$$

10. Finally, we extract $the\ mode$ l for the ith variable using the following formula (Eq. 10).

$$mode_i(q) = \emptyset\big((PC)(\mu)\big) \tag{10}$$

Where $\emptyset$ is the diagonal averaging product of PC and μ, q denotes the corresponding mode number. Figure 3 MDMD modes of different activities.

Improving the MDMD using the Hankel Matrix

The analysis and visualization of human activity are challenging research topics (Hu et al., 2020). Several decomposition-based techniques have been suggested to extract representative features from sensor data. The efficiency of extracted features strongly depends on the decomposition model and is often difficult to identify. In the context of human activity recognition (Kwon et al., 2014), we integrated the Hankel block and MDMD to improve the efficiency of extracted features. The MDMD is utilized to extract the dominant modes in time series data to analyze its behavior. However, this can be achieved when the sets of linearly independent of time series data with dominant modes contain a cardinality equal to or greater than the number of modes (Vasconcelos Filho & dos Santos, 2019). In other words, in some time series data, independencies occurred among the measured data which can prevent all modes from spanning. As a result, the DMDM could fail to correctly categorize system characteristics. To solve this issue, the Hankel matrix is employed. A Hankel matrix is a matrix with a constant with anti-diagonal. Suppose a time series $X = [x_1, x_2, x_3, \dots, x_n]$, the Hankel matrix H is constructed as (Eq. 11).

$$H = \begin{bmatrix} X_0 & X_1 & -- & X_n \\ X_1 & X_2 & -- & X_{n+1} \\ X_0 & X_0 & -- & X_0 \\ - & - & - & - \\ X_m & X_{m+1} & - & X_{m+n} \end{bmatrix} \tag{11}$$

Where the columns of the H correspond to all overlapping sub-sequences of the time series of length m, shifted by one element. This method redesigned the input of the time series data to create a new state variable.

Feature Extraction

In this paper, we extracted three frequency features and three statistical features from each MDMD mode. Several recent studies showed the ability of those features to reveal the hidden characteristics of time series data (Schmid, 2010; Suh et al., 2023). A total of 30 features (5X8) from each data row are extracted. In this section, a brief explanation is provided for each feature.

- **Mode frequency**: the dynamic mode oscillates at frequency f_{mod} is calculated from each mode and it was computed as (Eq. 12):

$$f_{mod} = Imag\left(\frac{\frac{\log(\rho)}{\Delta yt}}{2\pi}\right) \tag{12}$$

Where ρ represents the mode eigenvalue.

- **Power of mode:** the power of each mode is calculated and considered to recognize human activity. The main formula for the power of mode is expressed as (Eq. 13)**:**

$$Power_{mod} = \left(diag(Mode_i(q)^t Xmode_i\,(q)^t)\right) \tag{13}$$

- **Average of Absolute amplitude ($\boldsymbol{Abs\_Amp}$):** the Abs_Amp is computed for each mode, and it is expressed as (Eq. 14):

$$Abs_{Amp} = \frac{1}{N}\sum_{i=1}^{n}|mode_i(q)| \tag{14}$$

- **Variance:** it is employed to identify deviations in time series energy. It is calculated as follows (Eq. 15):

$$var = \frac{\sum(x_i - \bar{x})^2}{N-1} \tag{15}$$

Where: x_i represents an element of time series x, $\bar{x}$ is the mean of x, and N denotes the number of samples.

- **Skewness:** skewness is the third normalized central statistical moment. It measures the asymmetrical behavior of time series. The main formula of skewness is expressed as (Eq. 16)

$$skw = \frac{\sum_{i=1}^{N}(x_i-\bar{x})^3}{N\,\sigma_x^3} \tag{16}$$

- **Kurtosis:** it measures the peak value of the input time series. It is calculated as (Eq. 17):

$$x_{KURT} = \frac{\sum_{i=1}^{N}(x_i-\bar{x})^4}{N\sigma_x^4} \tag{17}$$

- **Approximate entropy (AEn)**: AEn measures the unpredictability and regularity of a sample using its past and current amplitude. Several research has shown that AEn is less influenced by noises. Suppose a time series data X of M datapoint, the AEN is calculated using as follows:

  1. First, the distance between any adjacent values $X(i)$, $X(j)$ in X is computed as follows: $Distance\ [X(i), X(j)\} = max[|X(i+r-1) - X(j+r-1)|]$
  2. Then, $y_i^m(r)$ is computed as $\mathrm{y_i^m(r)} = \frac{No.Of\ D[X(i),X(j)] \leq r}{n-m-1}$ where r is a threshold for value in X.
  3. Finally, the *AEn* is computed as follows (eq. 18 & 19)

$$AEn = \varphi^m(r) - \varphi^{m+1}(r) \tag{18}$$

Where $\varphi^m(r)$ is defined as

$$\varphi^m(kr) = \frac{1}{n-m-1}\sum_{i=1}^{n-m-1}\ln\left(\mathrm{y_i^m}\right) \tag{19}$$

- ***Shannon entropy (Shen)*:** it measures the uncertainty of a time series. The greater value of $Shen$ refers to the uncertainty and randomness of the time series. It is calculated as (eq. 20):

$$Shen = -\sum_{i=1}^{n} pro_i \ln(pro_i) \quad (20)$$

Where $Spro_i$ denotes the probability of the i value in the time series.

The Proposed Model Evaluation Approaches

In this paper, five statistical metrics were adopted for performance evaluation named Cohen's kappa precision, accuracy, f1-score, and recall. All metrics are described below:

- $Accuracy\ (Acc) = \frac{TP+TN}{TP+TN+FP+FN}$
- $Precsiion\ (PRE) = \frac{TP}{TP\_FP}$
- $Recall\ (REC) = \frac{TP}{TP+FN}$
- $F1 - score\ (F1) = \frac{2TP}{2TP+FP+FN}$
- $Cohens\ Kappa = \frac{p_0 - p_1}{1-p_0}$
- $Hamming\ loss\ (HLO) = \frac{1}{m.q}\sum_{i=1}^{m}\sum_{j=1}^{n}((h_j(x_i)) \neq y_{ij})$

Where $p_1 = \frac{\sum a_i b_i}{n^2}, p_0 = overall\ accuracy$, a_i the number of actual samples, and b_i id the number of classified samples.

Baseline Models

- **XGBoost**: Boosting was developed by Schapire (Zhang & Zhou, 2007). It creates an accurate classification model using a sequence of weak classifiers. In this study, we adopted the XGBoost algorithm as a benchmark. It belongs to the gradient Boosting machine algorithms (Qu et al., 2009). The training phase of each model in the XGboost algorithm is dependent on the previously trained models.
- **Stacking (Wei et al., 2018)** stacking is an ensemble method that was designed to solve multi-class classification problems. It’s like the Bagging ensemble that trains multiple base models on the original dataset. The base classifiers are used to generate classification using a testing set, then the classifications are used as input to a meta-learner to produce the final ensemble classification results.
- **Bagging (Schapire, 1990)**: Bagging is an ensemble method that was introduced to improve the accuracy of classification models by combining the results of multiple base models. It makes multiple bootstrap samples from the original dataset. Then it performs a random sampling with replacement to create subsets with a size like the original dataset. Each bootstrap sample is employed to train a separate bas classifier model. The final classification result is determined by a majority voting strategy.
- **Multi-label lazy learning (MLL)**: the model was designed based on the K-nearest neighbor (KNN) algorithm. For each unlabelled instance, its K nearest neighbors is identified using the training set. After calculating the number of neighbors for each instance belonging to one of the possible classes, the maximum a posteriori principle is employed to identify the label set for the unlabelled instance.

- **Weighted ensemble label-specific-features (LSFT)**: The proposed model in (Zhang & Zhou, 2007) can improve the performance of base learners. It generates multiple training sets using a bagging strategy.

3 Experiment and Dataset

Experimental datasets

A total of three HAR datasets named UCI-HAR, Opportunity, and WISDM were used for evaluation. The datasets are considered a benchmark for most human activity recognition models (Cho & Yoon, 2018). Table 1 delivers details of the datasets used in this paper (Duan et al., 2024; Chavarriaga et al., 2013; Anguita et al., 2013).

- **UCI-Human Activity Recognition**

The UCI- Human Activity recognition (An et al., 2021) dataset was acquired from 30 participants. The multivariate time-series data were recorded using a Samsung Galaxy mobile S2 smartphone with inertial sensors at a frequency rate of 50 Hz. The sensors were captured 3-axial linear accelerations and 3-axial angular velocities. Each subject performed six different activities including: upstairs sitting, downstairs, walking, lying, and standing.

- **Opportunity**

This dataset was recorded from four subjects four subjects. Five body sensors were placed on twelve positions on the upper part of the body and two were attached to shoes. Six activities per user were recorded where five activities were considered daily activities, and one was a drill run. This dataset included 18 different actions, and all data were sampled at a 30 Hz frequency. As mentioned in the previous studies, the Opportunity dataset contains an imbalance class distribution which represents 72.28% of the total samples (Balabka, 2019). In this study, subjects 1-3 were selected for the testing and the rest subjects were employed for training purposes. Three different actions were included in this dataset with the corresponding annotations.

- High-level activities: an example of these activities was taking a cup of tea, drilling, and relaxing. A total of six classes were adopted in this study. We also considered the null class.
- Mid-level gesture activities: these activities are produced from low-hand gestures. A total of 18 classes such as drinking, opening, and closing doors, including the null class.
- Low-level activities: these activities are walking, sitting, standing, etc. Five classes including null are considered in the simulation.

- **WISDM Dataset**

The WISDM dataset is published by Wireless Sensor Data Mining (WISDM). This dataset was recorded using a smartwatch and smartphone involving biometric sensors, accelerometers, and gyroscopes. Various basic activities including {*climbing stairs, jogging}* and eating activities *{eating chips, eating pasta}* and hand-based activities *{brushing teeth*, *and folding clothes*} were recorded in the WISDM dataset. To generate sensor time series, an embedded triaxial accelerometer was employed. All data was sampled at 20 Hz. A segmentation approach based on a sliding window was adopted to partition the data with a 95% overlap (0.5 s). We arbitrarily divided the data into 30% for the test set, and 70% for the training set.

Table 1: Physical Human Activity Datasets Description

Dataset	No. of classes and type of activity	Type of sensor	Sensor placement
Opportunity (Chavarriaga et al., 2013)	18 classes {daily living, drill}	12 acceleration, 7 inertial	2 on shoes, 5 upper body
UCI-HAR (Anguita et al., 2013)	6 classes {walking, sitting, standing}	3 angular, 3 linear accelerations	Smart Samsung phone on the waist
WISDM (Weiss et al., 2019)	7 classes {typing, jogging, …}	Accelerometer	Smartwatch, smartphone

Experimental Results

In this paper, we developed a human activity recognition model from WSN (Qi et al., 2019). The MDMD was employed with Hankel block coupled with ensemble classifiers. To demonstrate the effectiveness of the proposed model, we conducted several experiments using three datasets.

The Effect of Using the Hankel Matrix with MDMD on the Recognition Rate

In this paper, three datasets named Opportunity, UCI-HAR, and WISDM were utilized as benchmarks to evaluate the proposed MDMD-HB-DEM model. We selected different window sizes for each dataset. As a result, the window sizes were set as 10s, 5.21s, and 3s for the WISDM, and UCI-HAR Opportunity datasets respectively the human activity data was firstly passed through MDMD and then with an MDMD based on Hankel matrix. The selected features were sent into the proposed ensemble model. Table 2 summarizes the obtained results based on both approaches. It can be noticed that the MDMD provided good recognition results (Trajdos & Kurzynski, 2019), however, it failed to identify some complex activities. The main reason was that the MDMD produced similar features for some complex activities. Table 3 reports the results using MDMD with Hankel matrix. The recognition results were significantly improved using the Hankel matrix. The results confirmed the efficiency of integrating the MDMD with the Hankel matrix for human activity recognition.

We also calculated the confusion matrices, and the results were presented in Figure 2 for three datasets: Opportunity, UCI-HAR, and WISDM. From the results in Figure 2, it can be noticed that the proposed model performed very well with all datasets. The proposed model showed high recognition rates for simple physical activities and acceptable recognition rates for complex activities. However, with the Opportunity dataset (complex activities), there were some misclassified instances. The main reason for that it was found that the extracted features were very similar between complex classes in the Opportunity dataset.

Table 2: Recognition Results using Three Datasets Using MDMD

Dataset	Accuracy	Recall	Precision	f-score	kappa
Opportunity	0.8112	0.8013	0.8103	0.7902	0.7920
UCI-HAR	0.9421	0.9402	0.9316	0.9292	0.9164
WISDM	0.9012	0.9002	0.9001	0.8901	0.8851
Recognition results using three datasets using MDMD with Hankel matrix					
Opportunity	0.8832	0.8876	0.8806	0.8334	0.8102
UCI-HAR	0.9732	0.9783	0.9754	0.9381	0.9309
WISDM	0.9632	0.9542	0.9572	0.9382	0.926

UCI-HAR						
Laying	537	0	0	0	0	0
Sitting	7	468	17	0	0	0
Standing	0	22	513	0	0	0
Walking	0	0	0	495	0	0
Downstairs	2	0	1	0	417	0
Upstairs	0	0	2	2	4	463
	Laying	Sitting	Standing	Walking	Downstairs	Upstairs
Predicted						

WISDM						
Laying	1531	3	2	5	23	8
Sitting	6	5321	0	1	7	13
Standing	3	0	911	8	3	1
Walking	2	0	6	754	1	2
Downstairs	29	14	2	3	1805	12
Upstairs	10	9	1	4	9	6613
	Laying	Sitting	Standing	Walking	Downstairs	Upstairs
Predicted						

Opportunity (mode of locomotion)					
Standing	9575	197	12	0	65
Walking	31	491	0	0	116
Sitting	0	0	7646	108	27
Laying	0	0	0	804	8
Null	237	285	2	4	9201
	Standing	Walking	Sitting	Laying	Null
Predicted					

Opportunity (complex activity)						
Null	49	0	2	2	0	3
Relaxing	2	18	0	3	2	0
Cof_time	1	0	3	0	0	1
Ear_mg	3	5	0	135	0	3
cleanup	0	5	0	0	61	5
Sand_time	5	0	2	5	1	215
	null	Relaxing	Cof_time	Ear_mg	Cleanup	Sand_time
Predicted						

Figure 2: Confusion Matrix of Three Datasets

Comparison Against Benchmark Ensemble Models

The proposed dynamic ensemble model was compared against several benchmark ensemble models. For a fair comparison, the same hyperparameters in the previous studies were employed. The extracted features from Opportunity, UCI-HAR, and WISDM were sent to all ensemble classifiers. Tables 3-5 report the recognition results from three datasets. The best results were written in bold font.

The obtained results in Tables 3-5 confirmed that the proposed approach outperformed the previous ensemble models. It scored the highest accuracy, With the UCI-HAR dataset, the total number of classes was six, and the proposed model scored the highest recognition rates. Although there was a class imbalance problem associated with the WISDM dataset, the proposed model obtained a higher recognition rate than all models. In addition, some ensemble models showed high recognition rates such as LSF, LSFT, and XGBoost. It is noteworthy that the proposed model showed consistent accuracy with UCI-HAR and WISDM. The overall accuracy reached by the proposed model was accuracy=0.9732, 0.9532, f-score=0.9754, 0.9542, kappa=0.9781, 0.946, precision= 0.9709, 0.9582 for UCI-HAR, and WISDM respectively. The second-highest accuracy was recorded by LSFT. The LSFT model obtained an average accuracy of 0.9062, 0.9043, and an f-score of 0.9154, and 0.9032 for WISDM and UCI-HAR. Our goal was to design a generalized approach to recognize physical activities with a minimum error rate. In this experiment, we tested the proposed model with simple, and complex activities.

With the Opportunity dataset, the more complexity classes, our model performance was not as good as with WISDM and UCI-HAR as there were severely imbalanced classes, but it also gave better performance than the state-of-the-art models. The proposed model scored a high recognition rate on the Opportunity dataset for both complex and simple classes in terms of all metrics. The results showed that the proposed methods maintained good performances over three datasets, as indicated by the evaluation metrics. The receiver operating characteristics (ROC) curves were adopted for further evaluation. ROC curves reflect the correlations between false negative rate, true negative rate, and true positive rate. Figure. 3 depicts the ROC plots of all models. From the results scored in Figure 3, it was noticed that the proposed model correctly categorized most of the activities.

Table 3: Recognition Results Using the WISDM Dataset

Model	Accuracy	f-score	Recall	Precision	kappa
XGBoost	0.8822	0.8733	0.8824	0.8746	0.8657
Bagging	0.8532	0.85004	0.8498	0.8510	0.8421
Stacking	0.8976	0.89432	0.8905	0.8996	0.8876
LSFT	0.9043	0.9043	0.9092	0.9043	0.9032
MLL	0.7861	0.7851	0.7850	0.7842	0.7708
The proposed model	**0.9532**	**0.9542**	**0.9572**	**0.9582**	**0.946**

Table 4: Recognition Results Using the Opportunity Dataset

Model	Accuracy	f-score	Recall	Precision	kappa
XGBoost	0.8075	0.8124	08067	0.7976	0.7943
Bagging	0.7942	0.7765	0.7965	0.7865	0.7904
Stacking	0.8143	0.8154	0.8154	0.8152	0.8178
LSFT	0.8062	0.8124	0.8132	0.8163	0.8154
MLL	0.7443	0.7431	0.7846	0.7431	0.7431
The proposed model	**0.8832**	**0.8876**	**0.8806**	**0.8834**	**0.8802**

Table 5: Recognition Results Using the UCI-HAR Dataset

Model	Accuracy	f-score	Recall	Precision	kappa
XGBoost	0.9065	0.9043	0.9043	0.9061	0.9053
Bagging	0.8876	0.8843	0.8852	0.8854	0.8854
Stacking	0.9054	0.9076	0.9043	0.9054	0.9054
LSFT	0.8954	0.8954	0.8954	0.8943	0.8876
MLL	0.8651	0.8685	0.8543	0.8643	0.8543
The proposed model	**0.9732**	**0.9783**	**0.9754**	**0.9781**	**0.9709**

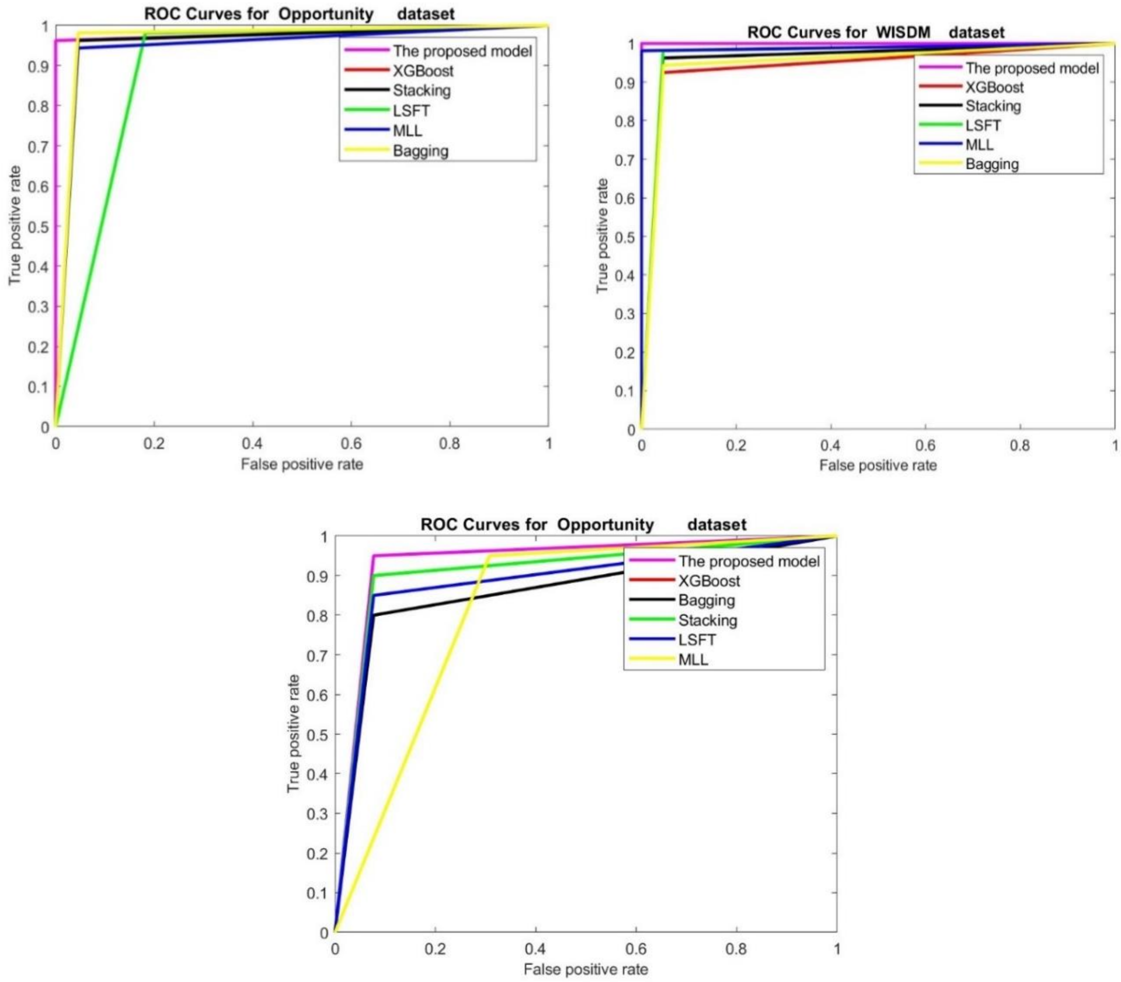

Figure 3: ROC Curves for all Models Using Three Datasets

4 Conclusions

In this study, we suggested an intelligent physical human activity recognition method (Tang et al., 2020). The proposed model integrated MDMD, Hankel block matrix, and a dynamic ensemble. Our finding showed that integrating the DMDM with the Hankel matrix improves the classification accuracy as the Hankel matrix expands the number of estimated modes. We also designed a dynamic ensemble model to address the unlabelled dataset problems. The MDMD was employed for the analysis of the time series data, while the ensemble model was used to address the challenge of unlabelled data. The study used wearable sensor data from three datasets to evaluate the proposed model. The obtained results were compared against several previous works. Our results show that the proposed model was more powerful and efficient for sensor-based physical human activity recognition.

References

[1] Abuhoureyah, F. S., Wong, Y. C., & Isira, A. S. B. M. (2024). WiFi-based human activity recognition through wall using deep learning. *Engineering Applications of Artificial Intelligence*, *127*, 107171. https://doi.org/10.1016/j.engappai.2023.107171

[2] Ahmadian, S., Rostami, M., Farrahi, V., & Oussalah, M. (2024). A novel physical activity recognition approach using deep ensemble optimized transformers and reinforcement learning. *Neural Networks*, *173*, 106159. https://doi.org/10.1016/j.neunet.2024.106159

[3] Ahmed, M., & Pandey, S. K. (2024). Digital Innovation Management: A Study of How Firms Generate and Implement Digital Ideas. *Global Perspectives in Management*, *2*(3), 13-23.

[4] An, S., Medda, A., Sawka, M. N., Hutto, C. J., Millard-Stafford, M. L., Appling, S., ... & Inan, O. T. (2021). AdaptNet: Human activity recognition via bilateral domain adaptation using semi-supervised deep translation networks. *IEEE Sensors Journal*, *21*(18), 20398-20411. https://doi.org/10.1109/JSEN.2021.3095176

[5] Anguita, D., Ghio, A., Oneto, L., Parra, X., & Reyes-Ortiz, J. L. (2013, April). A public domain dataset for human activity recognition using smartphones. In *Esann*, *3*(1), 3-4.

[6] Armstrong, D., & Tanaka, Y. (2025). Boosting Telemedicine Healthcare Assessment Using Internet of Things and Artificial Intelligence for Transforming Alzheimer's Detection. *Global Journal of Medical Terminology Research and Informatics*, *2*(1), 8-14.

[7] Bai, L., Yeung, C., Efstratiou, C., & Chikomo, M. (2019, September). Motion2Vector: Unsupervised learning in human activity recognition using wrist-sensing data. In *Adjunct proceedings of the 2019 ACM international joint conference on pervasive and ubiquitous computing and proceedings of the 2019 ACM international symposium on wearable computers* (pp. 537-542). https://doi.org/10.1145/3341162.3349335

[8] Balabka, D. (2019, September). Semi-supervised learning for human activity recognition using adversarial autoencoders. In *Adjunct proceedings of the 2019 ACM international joint conference on pervasive and ubiquitous computing and proceedings of the 2019 ACM international symposium on wearable computers* (pp. 685-688). https://doi.org/10.1145/3341162.3344854

[9] Bursa, S. O., Incel, O. D., & Alptekin, G. I. (2023). Personalized and motion-based human activity recognition with transfer learning and compressed deep learning models. *Computers and Electrical Engineering*, *109*, 108777. https://doi.org/10.1016/j.compeleceng.2023.108777

[10] Chavarriaga, R., Sagha, H., Calatroni, A., Digumarti, S. T., Tröster, G., Millán, J. D. R., & Roggen, D. (2013). The Opportunity challenge: A benchmark database for on-body sensor-based activity recognition. *Pattern Recognition Letters*, *34*(15), 2033-2042. https://doi.org/10.1016/j.patrec.2012.12.014

[11] Cho, H., & Yoon, S. M. (2018). Divide and conquer-based 1D CNN human activity recognition using test data sharpening. *Sensors*, *18*(4), 1055. https://doi.org/10.3390/s18041055

[12] Ding, W., Abdel-Basset, M., & Mohamed, R. (2023). HAR-DeepConvLG: Hybrid deep learning-based model for human activity recognition in IoT applications. *Information Sciences*, *646*, 119394. https://doi.org/10.1016/j.ins.2023.119394

[13] Diykh, M., Abdulla, S., Deo, R. C., Siuly, S., & Ali, M. (2023). Developing a novel hybrid method based on dispersion entropy and adaptive boosting algorithm for human activity recognition. *Computer Methods and Programs in Biomedicine*, *229*, 107305. https://doi.org/10.1016/j.cmpb.2022.107305

[14] Duan, H., Wang, S., Ojha, V., Wang, S., Huang, Y., Long, Y., ... & Zheng, Y. (2024). Wearable-based behaviour interpolation for semi-supervised human activity recognition. *Information Sciences*, *665*, 120393. https://doi.org/10.1016/j.ins.2024.120393

[15] Faye, S., Louveton, N., Gheorghe, G., & Engel, T. (2016). A two-level approach to characterizing human activities from wearable sensor data. *Journal of Wireless Mobile Networks, Ubiquitous Computing, and Dependable Applications, 7*(3), 1-21.

[16] Gao, W., Zhang, L., Teng, Q., He, J., & Wu, H. (2021). DanHAR: Dual attention network for multimodal human activity recognition using wearable sensors. *Applied Soft Computing*, *111*, 107728. https://doi.org/10.1016/j.asoc.2021.107728

[17] Hu, Y., Zhang, X. Q., Xu, L., He, F. X., Tian, Z., She, W., & Liu, W. (2020). Harmonic loss function for sensor-based human activity recognition based on LSTM recurrent neural networks. *IEEE Access*, *8*, 135617-135627. https://doi.org/10.1109/ACCESS.2020.3003162

[18] Hur, T., Bang, J., Huynh-The, T., Lee, J., Kim, J. I., & Lee, S. (2018). Iss2Image: A novel signal-encoding technique for CNN-based human activity recognition. *Sensors*, *18*(11), 3910. https://doi.org/10.3390/s18113910

[19] Hussain, A., Khan, S. U., Rida, I., Khan, N., & Baik, S. W. (2024). Human centric attention with deep multiscale feature fusion framework for activity recognition in Internet of Medical Things. *Information Fusion*, *106*, 102211. https://doi.org/10.1016/j.inffus.2023.102211

[20] Jethanandani, M., Sharma, A., Perumal, T., & Chang, J. R. (2020). Multi-label classification based ensemble learning for human activity recognition in smart home. *Internet of Things*, *12*, 100324. https://doi.org/10.1016/j.iot.2020.100324

[21] Kang, J., Kim, J., & Sohn, M. (2019). Supervised learning-based Lifetime Extension of Wireless Sensor Network Nodes. *Journal of Internet Services and Information Security*, *9*(4), 59-67.

[22] Kumar, A., Joshi, P., Bala, A., Sudhakar Patil, P., Jang Bahadur Saini, D. K., & Joshi, K. (2023). Smart Transaction through an ATM Machine using Face Recognition. *Indian Journal of Information Sources and Services*, *13*(2), 7–13. https://doi.org/10.51983/ijiss-2023.13.2.3752

[23] Kwon, Y., Kang, K., & Bae, C. (2014). Unsupervised learning for human activity recognition using smartphone sensors. *Expert Systems with Applications*, *41*(14), 6067-6074. https://doi.org/10.1016/j.eswa.2014.04.037

[24] Lu, Y., Wei, Y., Liu, L., Zhong, J., Sun, L., & Liu, Y. (2017). Towards unsupervised physical activity recognition using smartphone accelerometers. *Multimedia Tools and Applications*, *76*, 10701-10719. https://doi.org/10.1007/s11042-015-3188-y

[25] Ma, H., Zhang, Z., Li, W., & Lu, S. (2021). Unsupervised human activity representation learning with multi-task deep clustering. *Proceedings of the ACM on Interactive, Mobile, Wearable and Ubiquitous Technologies*, *5*(1), 1-25. https://doi.org/10.1145/3448074

[26] Menaka, S. R., Gokul Raj, M., Elakiya Selvan, P., Tharani Kumar, G., & Yashika, M. (2022). A Sensor based Data Analytics for Patient Monitoring Using Data Mining. *International Academic Journal of Innovative Research*, *9*(1), 28–36. https://doi.org/10.9756/IAJIR/V9I1/IAJIR0905

[27] Moya Rueda, F., Grzeszick, R., Fink, G. A., Feldhorst, S., & Ten Hompel, M. (2018, May). Convolutional neural networks for human activity recognition using body-worn sensors. In *Informatics, 5*(2), p. 26. MDPI. https://doi.org/10.3390/informatics5020026

[28] Ordóñez, F. J., & Roggen, D. (2016). Deep convolutional and lstm recurrent neural networks for multimodal wearable activity recognition. *Sensors*, *16*(1), 115. https://doi.org/10.3390/s16010115

[29] Patricia, A. C. P., Rosberg, P. C., Butt-Aziz, S., Alberto, P. M. M., Roberto-Cesar, M. O., Miguel, U. T., & Naz, S. (2024). Semi-supervised ensemble learning for human activity recognition in casas Kyoto dataset. *Heliyon*, *10*(8). https://doi.org/10.1016/j.heliyon.2024.e29398

[30] Qi, W., Su, H., Yang, C., Ferrigno, G., De Momi, E., & Aliverti, A. (2019). A fast and robust deep convolutional neural networks for complex human activity recognition using smartphone. *Sensors*, *19*(17), 3731. https://doi.org/10.3390/s19173731

[31] Qu, W., Zhang, Y., Zhu, J., & Qiu, Q. (2009). Mining multi-label concept-drifting data streams using dynamic classifier ensemble. In *Advances in Machine Learning: First Asian Conference on Machine Learning, ACML 2009, Nanjing, China, November 2-4, 2009. Proceedings 1* (pp. 308-321). Springer Berlin Heidelberg. https://doi.org/10.1007/978-3-642-05224-8_24

[32] Rahdar, A., Chahoushi, M., & Ghorashi, S. A. (2024). Efficiently improving the Wi-Fi-based human activity recognition, using auditory features, autoencoders, and fine-tuning. *Computers in Biology and Medicine*, *172*, 108232. https://doi.org/10.1016/j.compbiomed.2024.108232

[33] Raj, M. S., George, S. N., & Raja, K. (2024). Leveraging spatio-temporal features using graph neural networks for human activity recognition. *Pattern Recognition*, *150*, 110301. https://doi.org/10.1016/j.patcog.2024.110301

[34] Reddy, A. S. S., & Pachori, R. B. (2024). Multivariate dynamic mode decomposition for automatic imagined speech recognition using multichannel EEG signals. *IEEE Sensors Letters*, *8*(2), 1-4. https://doi.org/10.1109/LSENS.2024.3354288

[35] Saw, C. Y., & Wong, Y. C. (2023). Neuromorphic computing with hybrid CNN–Stochastic Reservoir for time series WiFi based human activity recognition. *Computers and Electrical Engineering*, *111*, 108917. https://doi.org/10.1016/j.compeleceng.2023.108917

[36] Schapire, R. E. (1990). The strength of weak learnability. *Machine learning*, *5*, 197-227. https://doi.org/10.1007/BF00116037

[37] Schmid, P. J. (2010). Dynamic mode decomposition of numerical and experimental data. *Journal of fluid mechanics*, *656*, 5-28. https://doi.org/10.1017/S0022112010001217

[38] Singh, S. P., Sharma, M. K., Lay-Ekuakille, A., Gangwar, D., & Gupta, S. (2020). Deep ConvLSTM with self-attention for human activity decoding using wearable sensors. *IEEE Sensors Journal*, *21*(6), 8575-8582. https://doi.org/10.1109/JSEN.2020.3045135

[39] Suh, S., Rey, V. F., & Lukowicz, P. (2023). Tasked: transformer-based adversarial learning for human activity recognition using wearable sensors via self-knowledge distillation. *Knowledge-Based Systems*, *260*, 110143. https://doi.org/10.1016/j.knosys.2022.110143

[40] Tang, Y., Teng, Q., Zhang, L., Min, F., & He, J. (2020). Layer-wise training convolutional neural networks with smaller filters for human activity recognition using wearable sensors. *IEEE Sensors Journal*, *21*(1), 581-592. https://doi.org/10.1109/JSEN.2020.3015521

[41] Trajdos, P., & Kurzynski, M. (2019). Dynamic classifier chains for multi-label learning. In *Pattern Recognition: 41st DAGM German Conference, DAGM GCPR 2019, Dortmund, Germany, September 10–13, 2019, Proceedings 41* (pp. 567-580). Springer International Publishing. https://doi.org/10.1007/978-3-030-33676-9_40

[42] Vasconcelos Filho, E., & dos Santos, P. L. (2019). A dynamic mode decomposition approach with hankel blocks to forecast multi-channel temporal series. *IEEE Control Systems Letters*, *3*(3), 739-744. https://doi.org/10.1109/LCSYS.2019.2917811

[43] Wang, H., Yang, J., Cui, C., Tu, P., Li, J., Fu, B., & Xiang, W. (2024). Human activity recognition based on local linear embedding and geodesic flow kernel on grassmann manifolds. *Expert Systems with Applications*, *241*, 122696. https://doi.org/10.1016/j.eswa.2023.122696

[44] Wei, X., Yu, Z., Zhang, C., & Hu, Q. (2018, July). Ensemble of label specific features for multi-label classification. In *2018 IEEE International Conference on Multimedia and Expo (ICME)* (pp. 1-6). IEEE. https://doi.org/10.1109/ICME.2018.8486444

[45] Weiss, G. M., Yoneda, K., & Hayajneh, T. (2019). Smartphone and smartwatch-based biometrics using activities of daily living. *IEEE Access*, *7*, 133190-133202. https://doi.org/10.1109/ACCESS.2019.2940729

[46] Xia, Q., Korpela, J., Namioka, Y., & Maekawa, T. (2020). Robust unsupervised factory activity recognition with body-worn accelerometer using temporal structure of multiple sensor data motifs. *Proceedings of the ACM on Interactive, Mobile, Wearable and Ubiquitous Technologies*, *4*(3), 1-30. https://doi.org/10.1145/3411836

[47] Xu, C., Chai, D., He, J., Zhang, X., & Duan, S. (2019). InnoHAR: A deep neural network for complex human activity recognition. *IEEE Access*, *7*, 9893-9902. https://doi.org/10.1109/ACCESS.2018.2890675

[48] Zahin, A., Tan, L. T., & Hu, R. Q. (2019). Sensor-based human activity recognition for smart healthcare: A semi-supervised machine learning. In *Artificial Intelligence for Communications and Networks: First EAI International Conference, AICON 2019, Harbin, China, May 25–26, 2019, Proceedings, Part II 1* (pp. 450-472). Springer International Publishing. https://doi.org/10.1007/978-3-030-22971-9_39

[49] Zhang, M. L., & Zhou, Z. H. (2007). ML-KNN: A lazy learning approach to multi-label learning. *Pattern recognition*, *40*(7), 2038-2048. https://doi.org/10.1016/j.patcog.2006.12.019

[50] Zhang, Q., Yuan, R., Lv, Y., Li, Z., & Wu, H. (2023). Multivariate dynamic mode decomposition and its application to bearing fault diagnosis. *IEEE Sensors Journal*, *23*(7), 7514-7524. https://doi.org/10.1109/JSEN.2023.3248285

[51] Zhao, Y., Yang, R., Chevalier, G., Xu, X., & Zhang, Z. (2018). Deep residual bidir-LSTM for human activity recognition using wearable sensors. *Mathematical problems in engineering*, *2018*(1), 7316954. https://doi.org/10.1155/2018/7316954

Authors Biography

Haydar Abdulameer Marhoon received his Ph.D. degree in Information Communication Technology, Computer Networks from UUM Malaysia, in 2017. His research and development experience includes over 15 years in area of research focuses on the Wireless Networking, Sensor Networking (WSN, WBAN, and IoT), Routing Protocols, Cloud, and Blockchain Technology.

Atheer Yousif oudah currently working as Assistant President for Administrative Affairs in Alayen Iraqi University. Atheer has completed his Master Degree in Information Technology from University Utara Malaysia in 2012 and his PhD in Computer science from Voronezh government University / Russia in 2019. His Research interest in Data Mining, Artificial Neural Network, Artificial Intelligence.

Naseer Ali Hussien currently working as Assistant Dean for Administrative Affairs of Denstiry College in Alayen Iraqi University. Naseer has completed his PhD in Computer science from Utara University / Malaysia in 2013. His Research interest in Network performance, Wireless and mobile Ad Hoc Networks, Network Protocol Engineering and Network Applications.

Alubady Raaid received his Ph.D. degree in Information Technology/ Computer Networks from the Universiti Utara Malaysia, in 2017. Alubady is an assistant Prof at the College of Information Technology at the University of Babylon-Iraq and currently, he is Deputy Dean at Engineering Technical College, Al-Ayen University. Alubady's research and development experience includes over 20 years in the Academia. Raaid current area of research focuses on the Future Internet (ICN and NDN), Wireless Networking, Sensor Networking (WSN, WBAN, and IoT), Routing Protocols, Cloud, and Fog Computing, and Blockchain Technology.